J. CHEM. SOC. DALTON TRANS. 1986 729

Kinetics of Hydration of Calcium Sulphate Hemihydrate

Kinjiro Fujii and Wakichi Kondo*
National Chemical Laboratory for Industry, Tsukuba Research Centre, Yatabe, Ibaraki 305, Japan

The kinetics of hydration of α-$CaSO_4 \cdot 0.5H_2O$ has been studied by calorimetry, analysis of the liquid phase, measurement of the combined water, and electron microscopic observations. Hemihydrate particles dissolve immediately after mixing with water and subsequently form hydrated layers on their surfaces by intrusion of water molecules, which grow to a thickness of *ca.* 0.09 μm according to a parabolic law and then undergo destruction, when the dihydrate nuclei are generated for the first time. At this point in time, the induction period terminates, and subsequent hydration of hemihydrate proceeds in accordance with the previously proposed rate equation based on the dissolution–crystallization mechanism.

Previously, studies of the hydration of calcium sulphate hemihydrate have been made by visual observations of changes in conditions of particles after their mixing with water,[1,2] analysis of the calcium sulphate concentration in the liquid phase,[3,4] measurement of the fluidity of slurry,[5] and by calorimetry.[4,6–10] In order to elucidate the kinetics of the hydration reaction, calorimetry is a particularly useful technique and there have been a number of reports[4,6–10] on such measurements. Through analysis of the heat generation, the hydration of the hemihydrate has been explained, as a whole, by the dissolution–crystallization mechanism, and some rate equations derived based on this mechanism have already been proposed,[4,6,10–13] of which that of Schiller[6] appears to have been most strictly derived. However, as it has been pointed out by Ridge[11] that there is an induction period involved in the hydration process, it is questionable to explain the whole process of hemihydrate hydration solely by the dissolution–crystallization mechanism.

The present paper reports the results of a study concerned particularly with when and by what mechanism are generated the nuclei of dihydrate crystals through the hydration of calcium sulphate hemihydrate.

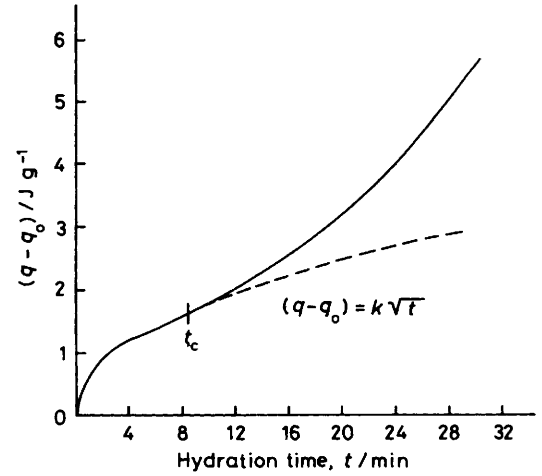

Figure 1. Heat evolved in the early stage of the hydration of α-$CaSO_4 \cdot 0.5H_2O$ at 20 °C and a water/hemihydrate mixing wt. ratio of 0.4; q = heat of hydration, observed; q_0 = heat of solution of α-$CaSO_4 \cdot 0.5H_2O$ in water

Experimental

Samples.—Coarse particles (0.1—0.5 mm) of high purity α-$CaSO_4 \cdot 0.5H_2O$, prepared in an autoclave, were ground to give particles of average diameter 40 μm (measured by Centrifugal Automatic Particle Analyser, Horiba CAPA-500) and having 6.62 wt.% of combined water which virtually coincides with the theoretical value. β-Calcium sulphate hemihydrate was also used in certain experiments; this was obtained by calcining the calcium sulphate dihydrate (plate-like crystals, size <250 μm) at 150 °C and had 8.54 wt.% of combined water.

Measurements.—The heat of hydration was measured by a twin-type conduction calorimeter (Tokyo Riko, model TCC-2). The combined water in the paste sample was quantitatively measured by removing free water using ethyl methyl ketone solvent, heating the sample and subjecting the released moisture to an analysis using a Karl–Fischer reagent.[14] The liquid phase in the paste was separated by absorption with a filter paper and the concentration of Ca^{2+} ion in the solution thus absorbed was measured after leaching out from the paper in accord with the chelate titration.[15] On the other hand, the change in the solid phase due to hydration was visually observed by a scanning electron microscope (Nippon Denshi, model JSM-15).

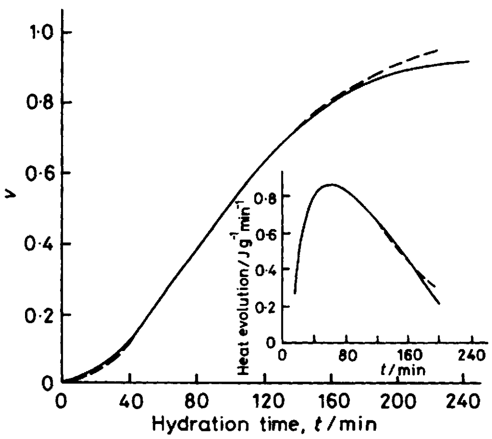

Figure 2. Progress (v = fraction of hemihydrate transformed to dihydrate) of hydration of α-$CaSO_4 \cdot 0.5H_2O$ at 20 °C, water/hemihydrate weight ratio 0.4, showing both observed (—) and calculated (- - -) curves. Inset shows the heat evolution rates

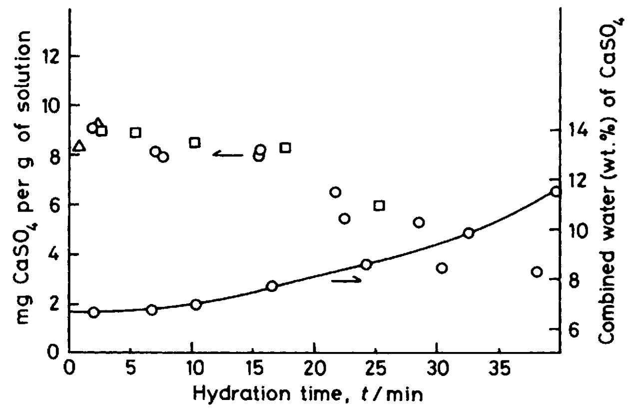

Figure 3. Concentration of CaSO$_4$ in the solution of hemihydrate paste and combined water content of the solid phase in the early stage at 20 °C. Water/hemihydrate weight ratios: (○) α, 0.4; (△) α, 1.0; (□) β, 1.0

Results

The relationship between the hydration time and the heat generated during the hydration is determinable from the rate of the heat generation. Figures 1 and 2 show the results for a paste having a water/hemihydrate weight ratio of 0.4 (20 °C). Figure 1 shows a curve of the heat generation obtained by subtracting from the total heat evolved, q, the dissolution heat, q_0 ($q_0 = 0.38$ J g^{-1}, see below). In Figure 2, the results are shown in the form of a conversion ratio of hemihydrate to dihydrate, this ratio being calculated using the heat of reaction for this transformation (129.1 J g^{-1}).[16,17] From Figure 1 it is seen that the curve of ($q - q_0$) follows a parabolic law for an initial period (to $t_c \approx 8.5$ min) and then deviates from it into an 'active stage'. Similar parabolic curves were reproduced in the six repeated experiments, though t_c varied in the range 6—9 min. After time t_c, as seen in Figure 2, the reaction follows a conventional sigmoid curve.

Turning to Figure 3, immediately after mixing of the hemihydrate with water the concentration of Ca^{2+} ion in the liquid phase of the paste is *ca.* 8.5 mg per g (about four times the solubility of the dihydrate) and *ca.* 10 min thereafter the concentration gradually diminishes. This tendency is observable also for the curve of the increase of bound water. Electron microscopic observations did not reveal any change in the appearance of the hemihydrate particles at an initial stage of the hydration (within *ca.* 6—7 min). It was noticeable, however, that after *ca.* 10 min the particles were fissured to form hair cracks in places on the surface, as shown in Figure 4(*a*), (*b*). Subsequently needle-like crystals of dihydrate were observed to grow not only on the outer surface of the particles but also inside as shown in Figure 4(*c*), (*d*). This surface layer may be a hydrated one formed in the initial period by superficial intrusion of water molecules as discussed later.

Discussion

Dissolution Heat when in Contact with Water and the Surface Condition of the Hemihydrate Particles.—The solubility (20 °C) of the α-hemihydrate is *ca.* 60 mmol kg^{-1} in water (8.2 mg CaSO$_4$ per g H$_2$O);[18] the data in Figure 3 are in close agreement. The heat of dissolution (ΔH_s) per mol of the hemihydrate is calculated by equation (1), where $\Delta H_f^{\ominus}$ and ΔH_f denote the standard enthalpy change and the enthalpy change respectively for the formation, suffixes CaSO$_4$(aq) or α-CaSO$_4$·0.5H$_2$O(s) denote the states of aqueous solution and solid, respectively; ΔH_f values are from the tables of Rossini *et al.*[19] [$\Delta H_{f,CaSO_4(aq)} = 1\,447.5$ kJ mol^{-1}]* and Babshkin *et al.*[16] [$\Delta H^{\ominus}_{f,CaSO_4\cdot 0.5H_2O(s)} = -1\,575.2$ kJ mol^{-1}].† Also, $\Delta H_{f,H_2O(aq)} \approx \Delta H^{\ominus}_{f,H_2O(l)}$. From these data, ΔH_s is calculated as -15.2 kJ mol^{-1}. Accordingly, the heat of dissolution (q_0) when the hemihydrate is mixed with water can be calculated by q_0 = (water/hemihydrate weight ratio) × (solubility) × ΔH_s. For example, if the water/hemihydrate weight ratios are 0.4 and 0.7, the q_0 values for 1 g of hemihydrate are 0.38 and 0.67 J respectively.

$$\Delta H_s = \Delta H_{f,CaSO_4(aq)} + 0.5\Delta H_{f,H_2O(aq)} - \Delta H^{\ominus}_{f,CaSO_4\cdot 0.5H_2O(s)} \quad (1)$$

If after the dissolution reaction [equation (2)] equilibrium is established between the hemihydrate particles and the aqueous solution, the equilibrium constant K can be calculated according to equations (3) and (4), where $\Delta G_f^{\ominus}$ is the standard free energy change for the formation of the compounds or ions in the subscript; γ and m are the activity coefficient and the molality. Respective $\Delta G_f^{\ominus}$ values at 298 K are known[16] and log K is thus -3.24 from equation (3). On the other hand, using the actually measured solubility of 60 mmol kg^{-1} in water and the $\gamma_{\pm}$ value of Gardner and Glueckauf,[21] log $K = -3.49$ is obtained. Thus, the calculated equilibrium constant is almost identical to that actually measured. This suggests that the hemihydrate shows a substantially genuine solubility immediately after its contact with water and the surface condition of the particles scarcely changes from the view-point of free energy as compared to that prior to mixing with water.

$$\alpha\text{-CaSO}_4\cdot 0.5H_2O \longrightarrow Ca^{2+}(aq) + SO_4^{2-}(aq) + 0.5H_2O \quad (2)$$

$$\Delta G^{\ominus}_{f,CaSO_4\cdot 0.5H_2O(s)} = \Delta G^{\ominus}_{f,Ca^{2+}(aq)} + \Delta G^{\ominus}_{f,SO_4^{2-}(aq)} + 0.5\Delta G^{\ominus}_{f,H_2O(l)} + RT \ln K \quad (3)$$

$$K = \gamma_{Ca^{2+}}\gamma_{SO_4^{2-}}m_{Ca^{2+}}m_{SO_4^{2-}} \quad (4)$$

Reaction During the Induction Period.—As shown in Figure 3, the concentration of the liquid phase is almost constant at the initial stage, therefore the heat generation ($q - q_0$) in Figure 1 can be ascribed to a intrusion reaction of water into the hemihydrate particles which follows the parabolic law (5), where t is the time and k is a constant equal to 0.55 J g^{-1} min$^{-\frac{1}{2}}$ (20 °C). This equation is applicable with good reproducilibity and suggests that the reaction is a similar tarnishing reaction to the oxidation of metal which proceeds accompanying the growth of the hydrated layer on the particle surfaces. However, as shown in Figure 1, the parabolic law is only satisfied up to $t_c \approx 8.5$ min. Before and after the time t_c, hair-like fissures are seen to occur sporadically, and this suggests that destructive changes probably occur in the hydrated layer. Thus, making the following assumptions, the thickness of the hydrated layer at this point can be calculated. If all of the hemihydrate particles (average radius of particle, $r = 20$ μm) uniformly form a layer,

$$q - q_0 = k\sqrt{t} \quad (5)$$

---

* In the table,[19] $\Delta H_{f,CaSO_4(aq)}$ values are given as a function of molality of CaSO$_4$, m, up to 22.2 mmol kg^{-1}, so by extrapolating the relationship between $\Delta H_{f,CaSO_4(aq)}$ and $\sqrt{m}$ the value at 60 mmol kg^{-1} was estimated.

† $\Delta H^{\ominus}_{f,CaSO_4\cdot 0.5H_2O(s)}$ is otherwise evaluated to be $-1\,576.7$ kJ mol^{-1} from the following data at 298 K: the heat of hydration of 17.15 kJ mol^{-1}[20] for α-CaSO$_4$·0.5H$_2$O(s) + 1.5H$_2$O(l) $\longrightarrow$ CaSO$_4$·2H$_2$O(s); $\Delta H^{\ominus}_{f,CaSO_4\cdot 2H_2O(s)} = -2\,022.63$,[17] $\Delta H^{\ominus}_{f,H_2O(l)} = -285.83$ kJ mol^{-1}.[17]

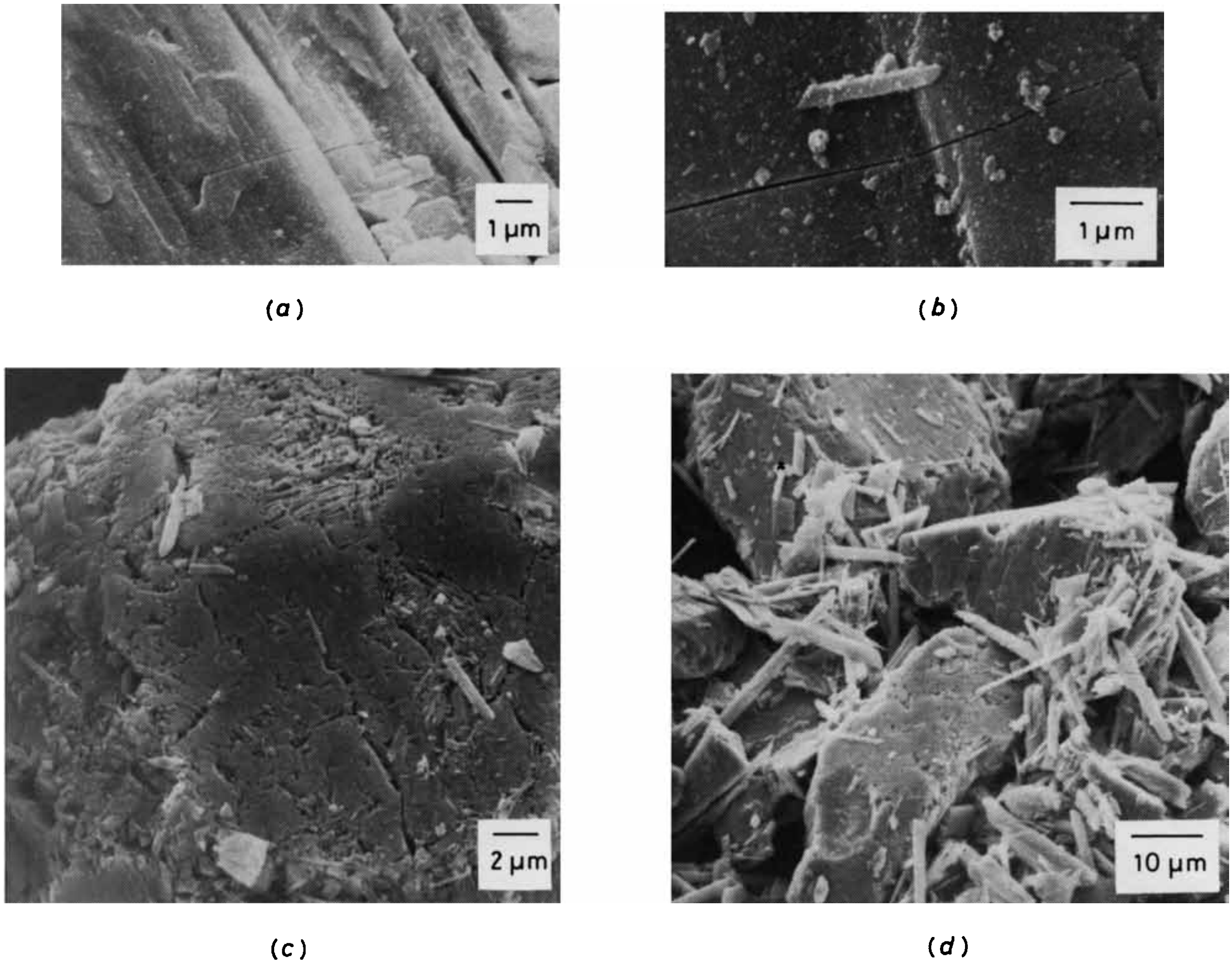

Figure 4. Specimens of α-$CaSO_4 \cdot 0.5H_2O$ paste: (*a*) and (*b*) aged 10 min at 20 °C (hair cracks were found sporadically); (*c*) and (*d*) aged 24 min (needle-like dihydrate grew both outside and inside of the surface coating)

the thickness (y) of the reacted layer can be recalculated by equation (6), where v is the conversion ratio. Further, on the

$$y = r[1 - (1 - v)^{\frac{1}{3}}] \qquad (6)$$

assumption that the $(q - q_0)$ value in Figure 1 is due to the formation of the crystalline dihydrate, as a first approximation $(q - q_0)$ up to the time t_c is 1.67 J g^{-1} and thus $v = 1.67/129.1 = 0.013$. Therefore, $y = 0.087$ µm. The difference in molar volume between the hemihydrate and dihydrate is considered as a factor in whether destruction of the layer would occur by the growth of such a thin hydrated layer. The molar volumes are 52.97 cm^3 mol^{-1} and 74.21 cm^3 mol^{-1}, respectively; when the hemihydrate is transformed to dihydrate a 40% volume expansion (12% linear expansion) will occur. This means that a large compressive stress is produced in the surface layer of hemihydrate particles through superficial intrusion of water molecules. Reflecting this effect, the solution, which is quasi-equilibrated with thus superficially 'intrusion-hydrated' particles, maintains a high [$CaSO_4$] (as seen in Figure 3) during the induction period. When this stress is released by destruction of the layer, the nuclei of dihydrate are formed. Accordingly, it may be said that the nuclei of dihydrate are generated for the first time when the intrusion-hydrated layer formed on the surface of hemihydrate particles reaches a certain critical thickness (0.087 µm), and that neither are they inherently present on the surface of the hemihydrate particles[6] nor are they generated by fluctuation of the free energy of the hemihydrate particles.[8] Further, the intrusion-hydrated layer during the induction period may be an amorphous layer which is thought to correspond to the colloidal layer proposed by Eipeltauer.[1]

Main Reaction based on the Dissolution–Crystallization Mechanism.—As shown in Figure 2, the hydration is accelerated from the time t_c and, as a whole, follows a sigmoid conversion curve. With respect to such a process, Schiller[3,6,7] proposed that when the nuclei of dihydrate undergo crystalline growth with Ca^{2+} ions and $SO_4{}^{2-}$ ions supplied through the dissolution of the hemihydrate, the transportation of these substances is driven by the difference in solubility between both phases, and proposed equation (7), where t and v are

$$t = K_1 v^{\frac{1}{3}} + K_2[1 - (1 - v)^{\frac{1}{3}}] \qquad (7)$$

respectively the time and the conversion ratio; K_1 and K_2 are parameters both dependent on the water/hemihydrate weight ratio of the slurry and the difference in solubility between the hemihydrate and the dihydrate. K_1 also depends on the number of the nuclei of the dihydrate, while K_2 also depends on the fineness of the hemihydrate particles and the dissolution rate constant.

Equation (7) has been proposed, assuming that the nuclei of dihydrate are inherently present in the hemihydrate sample. In this case, v will increase in proportion to t^3 at the initial stage of the hydration. On the contrary, when these nuclei are generated for the first time at the critical point t_c in Figure 1, as in the case of the α-hemihydrate used in the present experiments, it is necessary to use the two equations (8) and (9) for the

$$t_c \geqslant t \geqslant 0 \qquad v = v_o + k'\sqrt{t} \qquad (8)$$

$$t \geqslant t_c \qquad t - t_c = K_1(v - v_c)^{\frac{1}{3}} + K_2\{1 - [1 - (v - v_c)]^{\frac{1}{3}}\} \qquad (9)$$

$$t \geqslant t_c \qquad dv/dt = 3\{K_1(v - v_c)^{-\frac{2}{3}} + K_2[1 - (v - v_c)]^{-\frac{2}{3}}\}^{-1} \qquad (10)$$

conversion–time relation, drawing a line of demarcation at t_c. The conversion ratio v_o corresponds to the portion of the hemihydrate dissolved in water immediately after contacting with water and v_c is the conversion at the end of the induction period, t_c. In addition, equation (10) indicates the rate of hydration after t_c, as derived from equation (9).

From the observed curve (solid line) in Figure 2, parameters K_1 and K_2 are determined to be 44 and 276 min, respectively. Further, it is understood that the curves calculated from equations (9) and (10) using these values (broken lines in Figure 2) follow well the observed curve.

Acknowledgements

We thank Mr. H. Azuma, Mr. S. Sakai, and Mr. N. Hidaka for their co-operation in carrying out these experiments and also Ms. J. Tanaka for her help in the preparation of this paper.

References

1 E. Eipeltauer, *Zem.-Kalk-Gips*, 1963, **16**, 9.
2 A. N. Knauf, W. Kronert, and P. Haubert, *Zem.-Kalk-Gips*, 1972, **25**, 546.
3 K. Schiller, *J. Appl. Chem.*, 1965, **15**, 581.
4 C. Comel, E. Karmazsin, and M. Murat, *Thermochim. Acta*, 1979, **31**, 71.
5 G. Neuhauser, *Zem.-Kalk-Gips*, 1975, **29**, 227.
6 K. Schiller, *J. Appl. Chem.*, 1962, **12**, 135.
7 K. Schiller, *J. Appl. Chem. Biotechnol.*, 1974, **24**, 379.
8 E. C. Combe, D. C. Smith, and M. Braden, *J. Appl. Chem.*, 1970, **20**, 287.
9 O. Matsuda, *Sekko To Sekkai*, 1982, **117**, 74.
10 E. Karmazsin, C. Comel, and M. Murat, *Cim. Beton Platres Chaux*, 1983, **740**, 47.
11 M. J. Ridge, *Nature (London)*, 1964, **204**, 70.
12 J. H. Taplin, *Nature (London)*, 1965, **205**, 864.
13 J. H. Taplin, *J. Appl. Chem. Biotechnol.*, 1973, **23**, 349.
14 K. Fujii and W. Kondo, *J. Am. Ceram. Soc.*, 1974, **57**, 492.
15 K. Fujii and W. Kondo, Proc. 5th Int. Symp. Chem. Cement, Tokyo, 1968, vol. 2, p. 362.
16 V. I. Babshkin, G. M. Matveev, and O. P. Mchedlov-Petrosyan, 'Thermodynamics of Silicates,' 3rd rev. and suppl. edn., Publication of Construction Literature, Moscow, 1972, pp. 324—345.
17 R. A. Robie, B. S. Hemingway, and J. R. Fischer, 'Thermodynamic Properties of Minerals and Related Substances at 298.15 K and 1 Bar Pressure at Higher Temperatures,' Geological Survey Bull. 1452, U. S. Gov. Printing Office, Washington, 1979, pp. 12—29.
18 O. Knacke and W. Gans, *Z. Phys. Chem.*, 1977, **104**, 41.
19 F. D. Rossini, D. D. Wagman, W. H. Evans, S. Levine, and I. Jaffe, 'Selected Values of Chemical Thermodynamic Properties,' Nat. Bur. Stand., 1953, circular 500, p. 390.
20 J. C. Southard, *Ind. Eng. Chem.*, 1940, **32**, 442.
21 A. W. Gardner and E. Glueckauf, *Trans. Faraday Soc.*, 1970, **66**, 1081.

Received 5th *March* 1985; *Paper* 5/372